

Supporting Information

**A screening of properties and application based on  
dimerized fused-ring non-fullerene acceptors: Influence of  
C=C, C-C, *spiro*-C linkers**

Ming-Yue Sui,<sup>\*a</sup> Song Xiao,<sup>a</sup> Fei Wang,<sup>b</sup> Guang-Yan Sun<sup>\*a, c</sup>

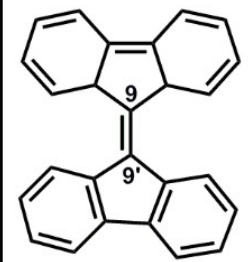
<sup>a</sup> Department of Chemistry, Faculty of Science, Yanbian University, Yanji, Jilin, 133002, China. \*E-mail: [0000008661@ybu.edu.cn](mailto:0000008661@ybu.edu.cn)

<sup>b</sup> Departament de Química Física i Inorganica, Universitat Rovira i Virgili, c/Marcel·lí Domingo 1, Tarragona, 43007, Spain.

<sup>c</sup> Faculty of Chemical Engineering and New Energy Materials, Zhuhai College of Jilin University, Zhuhai, Guangdong, 519041, China.

## Section 1. Supplementary description

Structural and property characteristics of **BF**:

	<ul style="list-style-type: none"><li>i) Twisted structure—inhibits larger phase separation</li><li>ii) C=C core—facilitate the delocalization, enhance electronic coupling, control excitation energies</li><li>iii) Many different substitution functional sites</li><li>iv) easy to accept an electron to satisfy Hückel's requirements and 14-<math>\pi</math>-electron aromaticity</li><li>v) singlet fission character</li><li>vi) exhibit excellent plasticity to compensate defects of peripheral units</li></ul>
---	---

A literature review about **BF**-based nonfullerene acceptors:

Compared to PDI and ITIC derivatives, there is limited research on **BF**-based in non-fullerene small molecule acceptor (SMA) materials. Since **BF** as an electron acceptor was reported (Angew. Chem. Int. Ed., 2010, 49, 532-536), we have found that if only the **BF** monomer molecule was used as SMA, the performance of device is generally lower (the maximum PCE value is 2.28%, which is limited by  $J_{SC}$ , but  $V_{OC}$ s are both higher, both greater than 1.0 V) (Chem. Commun., 2013, 49 10950-10952). However, with **BF** as the core unit, SMA could exhibit excellent plasticity. It would compensate for the structure or performance defects of peripheral units, and try to maintain the superior properties of both units. For example, introducing **BF** as core unit in NDI materials could solve its poor morphological stability (RSC Adv., 2016, 6, 70493-70500); applying in PDI could effectively inhibit the excessive self-aggregation of PDI materials, and form favorable phase separation in blend films (Chem. Eur. J. 2018, 24, 4149-4156). As the number of peripheral unit's increases, the performance of the device is significantly improved, achieving an effective superposition of molecular properties. As a result, the PCE of P3HT:H1 reaches 5.42%, which is among the best efficiencies achieved with P3HT as the donor polymer (New J. Chem., 2017, 41, 6822-6827). All of the above demonstrate the infinite potential of the **BF** monomer in performance-regulating hinge and application. However, the maximum PCE of the **BF** based OPV device is 5.95% to date, which may be due to the lack of matching and compatible peripheral connection units (this is also the direction we are working hard) and less research attempts. Importantly, the structure and performance modification rules of **BF** core are not still clear to date. This is one of the purposes of this work (J. Mater. Chem. C, 2017, 5, 4909-4914; J. Org. Chem. Front., 2017, 4, 650-657; J. Mater. Chem. C, 2017, 5, 10343-10352; J. Phys. Chem. A, 2014, 118, 5961-5968; J. Phys. Chem. C, 2019, 123, 11397-11405).

## Section 2. Tables and Figures

Figures:

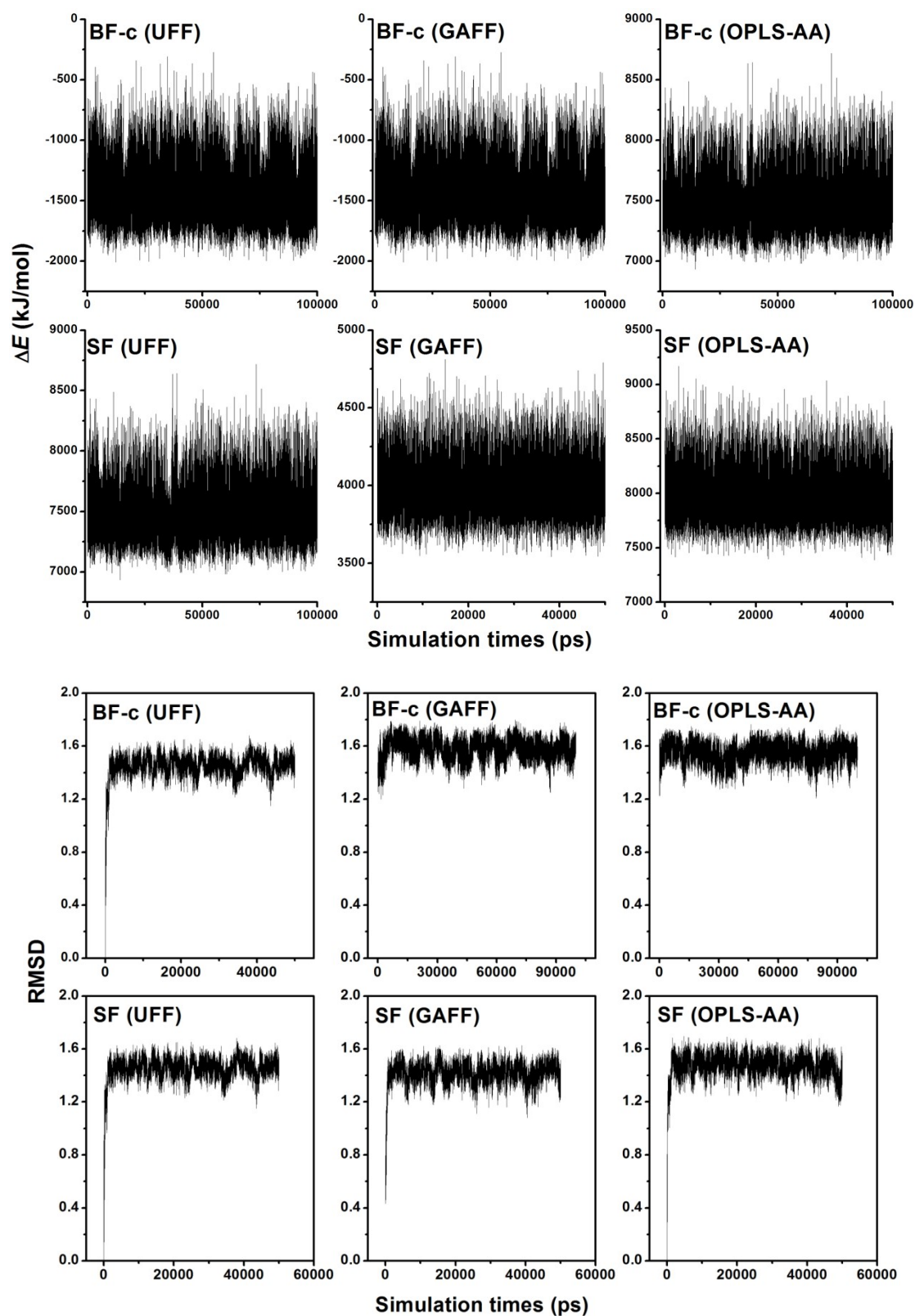


Figure S1. The plots of the potential energies and RMSD in **BF-c** and **SF** aggregates employing UFF, GAFF and OPLS-AA force field versus simulation times for MD process.

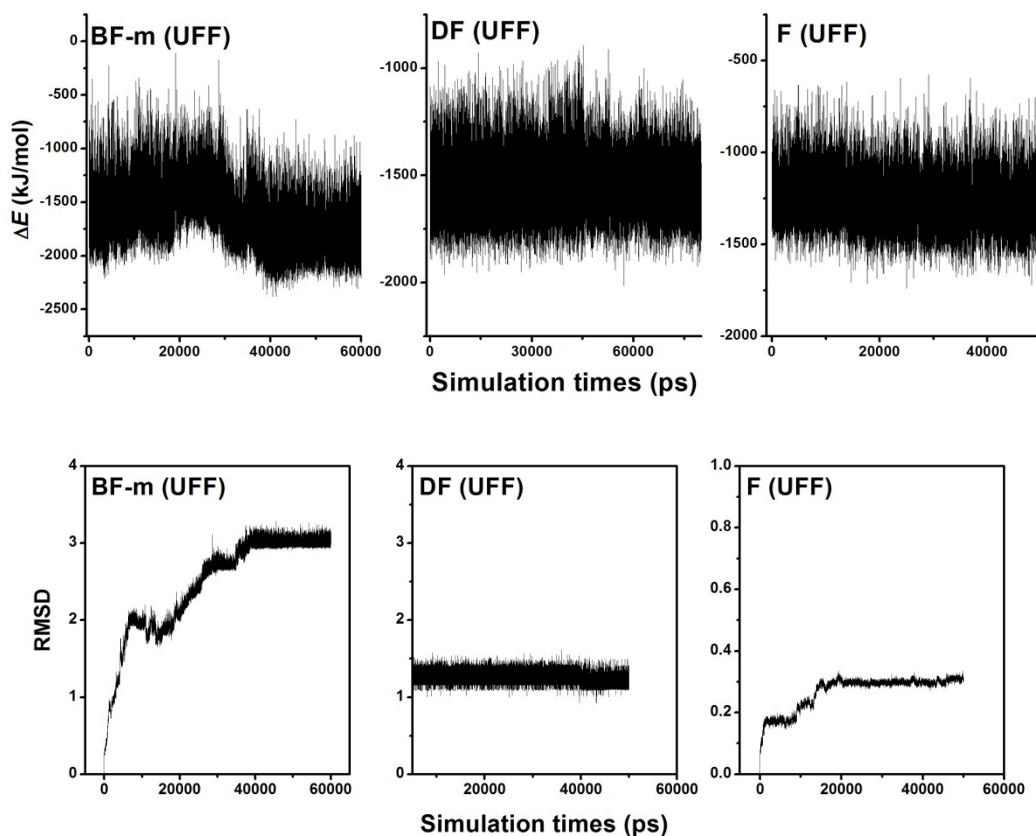


Figure S2. The plots of the potential energies and RMSD in **BF-m**, **DF** and **F** aggregates employing UFF force field versus simulation times for MD process.

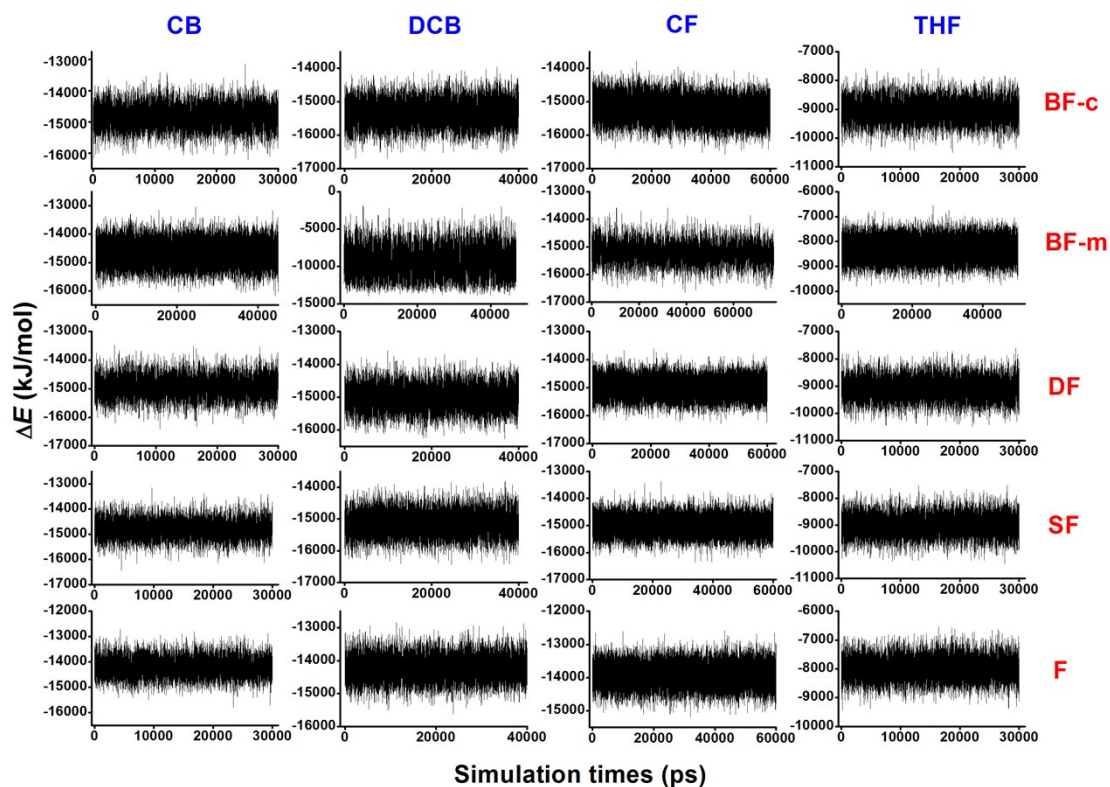


Figure S3. The plots of the potential energies in all systems immersed in four solvents aggregates versus simulation times for MD process.

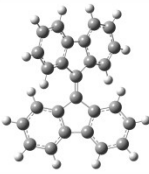

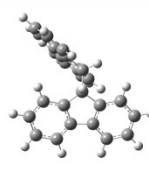

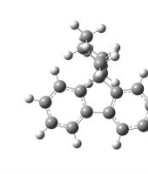
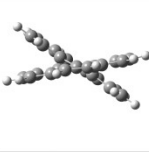
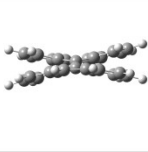
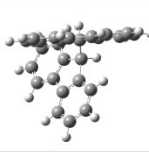

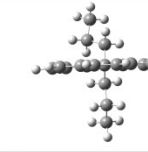
	BF-c	BF-m	DF	SF	F
Front View					
Bottom View					
$\omega$	33.98°	9.50°	69.94°	90.00°	

Figure S4. Optimized molecular structures and twist angles ( $\omega$ ) of all compounds in ground state.

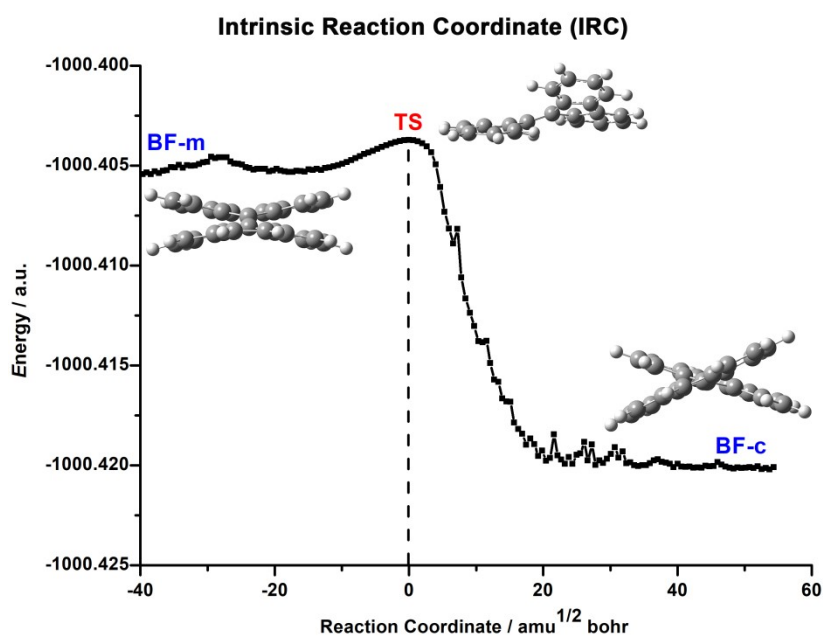


Figure S5. Structure formation energy profile vs. reaction coordinate using the LQA methods at the B3LYP/6-31G(d) level.

Figure S6: The centroid position of **BF** is overlap and located at the center of C=C, verifying C=C plays a leading role. For **DF**, the centroid position is up the center C-C, which indicates that C-C has a spatial effect in space on two fragments through its structural characteristics, while the connectivity of C-C itself is small. Based on the above conjecture of **SF** excitation characteristics, its centroid position is slightly separated in  $S_1$  state, asymmetrically located at both ends of *spiro*-

C, indicating its effect is uneven. In  $S_5$  and  $S_6$ , one centroid is located on *spiro-C* and the other is located on the edge of one five-membered ring. Based on the selectivity of fragment (two different directions), which form the degenerate states  $S_5$  and  $S_6$ .

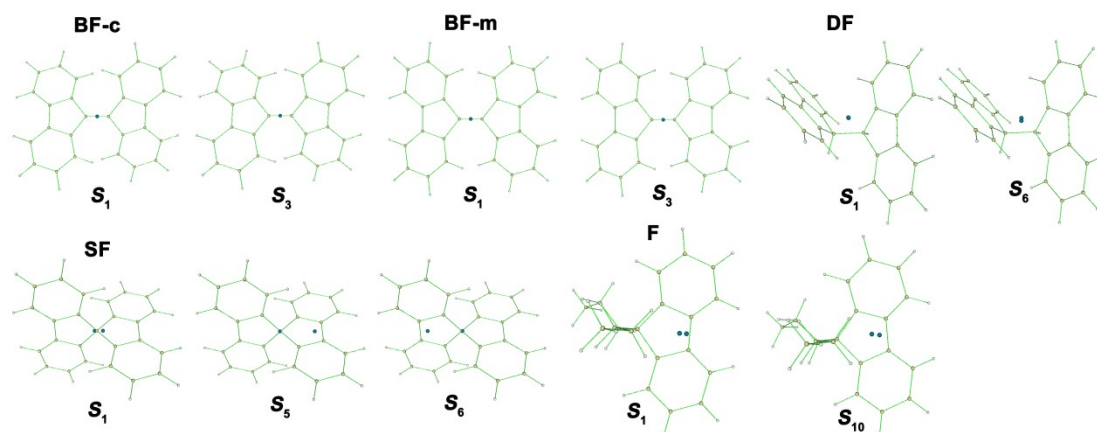


Figure S6. The centroid position of transitional orbitals on the major excited state.

 PDI $R_1 \sim R_4$	<b>R1</b>	<b>BF-c(PDI)<sub>1</sub></b>	<b>BF-m(PDI)<sub>1</sub></b>	<b>SF(PDI)<sub>1</sub></b>	<b>DF(PDI)<sub>1</sub></b>
	<b>R1,R2</b>	<b>BF-c(PDI)<sub>2-1</sub></b>	<b>BF-m(PDI)<sub>2-1</sub></b>	<b>SF(PDI)<sub>2-1</sub></b>	<b>DF(PDI)<sub>2-1</sub></b>
	<b>R1,R3</b>	<b>BF-c(PDI)<sub>2-2</sub></b>	<b>BF-m(PDI)<sub>2-2</sub></b>	<b>SF(PDI)<sub>2-2</sub></b>	<b>DF(PDI)<sub>2-2</sub></b>
	<b>R1~R3</b>	<b>BF-c(PDI)<sub>3</sub></b>	<b>BF-m(PDI)<sub>3</sub></b>	<b>SF(PDI)<sub>3</sub></b>	<b>DF(PDI)<sub>3</sub></b>
	<b>R1~R4</b>	<b>BF-c(PDI)<sub>4</sub></b>	<b>BF-m(PDI)<sub>4</sub></b>	<b>SF(PDI)<sub>4</sub></b>	<b>DF(PDI)<sub>4</sub></b>

Figure S7. The structure strategies with different dimerized fluorene cores and variational numbers of DPP groups at various positions.

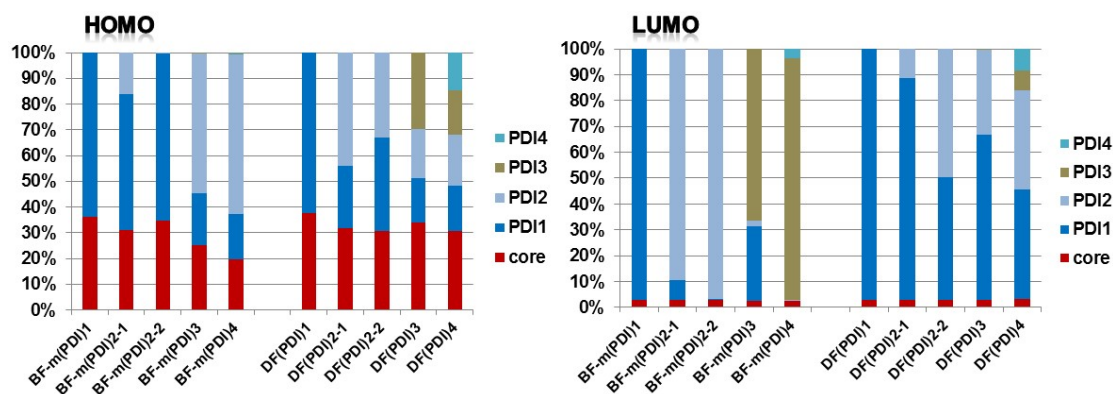


Figure S8. The HOMO and LUMO orbital compositions of each unit in **BF-m(PDI)<sub>i</sub>** and **DF(PDI)<sub>i</sub>** were analyzed by the Hirshfeld method.

### Tables:

Table S1. Calculated and experimental bond lengths (in Å), bond angles (in deg) and dihedral angles (in deg) of **BF-c** and **SF** at ground state (B3LYP/6-31G(d)).

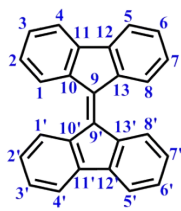
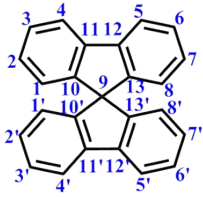
		Cal.	Exp.		Cal.	Exp.	
	<b>BF-c</b>	R(1,10)	1.400	1.397	R(11,12)	1.463	1.454
		R(1,2)	1.397	1.399	R(9,9')	1.381	1.367
		R(2,3)	1.399	1.371	A(10,9,13)	105.4	104.9
		R(3,4)	1.397	1.373	A(9,10,11)	109.0	109.1
		R(4,11)	1.393	1.394	A(10,11,12)	108.3	108.4
		R(9,10)	1.482	1.476	DA(10,9,9',10')	34.0	34.0
		R(10,11)	1.419	1.400			
	<b>SF</b>	R(1,10)	1.390	1.386	R(11,12)	1.469	1.475
		R(1,2)	1.410	1.404	R(12,13)	1.387	1.475
		R(2,3)	1.366	1.369	A(10,9,13)	100.9	101.2
		R(3,4)	1.382	1.387	A(9,10,11)	111.1	110.7
		R(4,11)	1.392	1.397	A(10,11,12)	108.2	109.1
		R(9,10)	1.527	1.536	A(10,9,10')	115.3	112.3
		R(10,11)	1.387	1.381			

Table S2. The Van der Waals radius of all molecules.

Solute	<b>BF-c</b>	<b>BF-m</b>	<b>DF</b>	<b>SF</b>	<b>F</b>
Van der Waals radius (nm)	1.38	1.42	1.40	1.18	1.18
Solvent	CB	DCB	CF	THF	
Van der Waals radius (nm)	0.86	0.86	0.65	0.65	

Table S3. Calculated the distances (Å) and dihedral angles  $\omega$  (°) between fluorenes for compounds with the B3LYP/6-31G (d) level.

	core	1-1'	8-8'	$\omega$
<b>BF-c</b>	1.38	3.21	3.21	33.98
<b>BF-m</b>	1.37	3.06	3.06	9.50
<b>DF</b>	1.56	3.87	3.87	69.94

SF                      0.00                      3.85                      3.85                      90.00

---

Table S4. Calculated maximum absorption peaks  $\lambda_{\max}$  (nm), oscillator strengths  $f$  and major configurations of the molecules at the TD-B3LYP/6-31G(d) level.

	states	$\lambda_{\max}$	$f$	composition <sup>a</sup>		
<b>BF-c</b>	$S_1$	471.4/458.0	0.000	H-1→L (99%)		
	$S_3$	463.5	0.473	H→L (100%)		
<b>BF-m</b>	$S_1$	429.7	0.001	H-1→L (99%)		
	$S_3$	392.1	0.514	H→L (99%)		
<b>DF</b>	$S_1$	279.1	0.029	H→L (77%)	H-1→L+1 (16%)	
	$S_6$	263.7	0.389	H-1→L (39%)	H→L+1 (45%)	
<b>SF</b>	$S_1$	290.1	0.053	H→L (78%)		H→L+1 (11%)
	$S_5$	263.8	0.168	H-2→L (10%)	H-1→L (54%)	H-1→L+1 (28%)
	$S_6$	263.8	0.168	H-2→L+1 (10%)	H-1→L (28%)	H-1→L+1 (54%)
<b>F</b>	$S_1$	269.7	0.257	H-2→L (10%)	H→L (74%)	H→L+1 (11%)
	$S_{10}$	189.2	0.636	H-2→L+1 (22%)		H-1→L+2 (66%)

<sup>a</sup> H denotes HOMO and L denotes LUMO.